Coupling Geometrically Exact Cosserat Rods and Linear Elastic Continua

Oliver Sander

Freie Universität Berlin, Fachbereich Mathematik und Informatik, Arnimallee 6, Berlin.
sander@mi.fu-berlin.de

UNCORRECTED PROOF

Summary. We consider the mechanical coupling of a geometrically exact Cosserat rod to a linear elastic continuum. The coupling conditions are formulated in the nonlinear rod configuration space. We describe a Dirichlet–Neumann algorithm for the coupled system, and use it to simulate the static stresses in a human knee joint, where the Cosserat rods are models for the ligaments.

1 Cosserat Rods and Linear Elasticity

Cosserat rods are models for long slender objects. Let $SE(3) = \mathbb{R}^3 \rtimes SO(3)$ be the group of orientation-preserving rigid body motions of $\mathbb{R}^3$ (the special Euclidean group). A configuration of a Cosserat rod is a map $\varphi : [0,1] \to SE(3)$. For each $s \in [0,1]$, the value $\varphi(s) = (\varphi_r(s), \varphi_q(s))$ is interpreted as the position $\varphi_r(s) \in \mathbb{R}^3$ and orientation $\varphi_q(s) \in SO(3)$ of a rigid rod cross section. Strain measures $(\mathbf{v}_\varphi(s), \mathbf{u}_\varphi(s))$ at $\varphi(s)$ live in the tangent space $T_{\varphi(s)}SE(3)$, and are defined by

$$\mathbf{v}_\varphi(s) = \varphi_r'(s) \qquad \text{and} \qquad \varphi_q'(s) = \mathbf{u}_\varphi^\times(s)\varphi_q(s),$$

where $\mathbf{u}_\varphi^\times$ is the skew-symmetric matrix corresponding to $\mathbf{u}_\varphi$. On each cross section s of the rod act a resultant force and torque. These are given by a tuple $(\mathbf{n}(s), \mathbf{m}(s))$, which is an element of the cotangent space $T^*_{\varphi(s)}SE(3)$. In the absence of external forces and torques we have the equations of equilibrium [6]

$$\begin{aligned} \mathbf{m}' + \varphi_r' \times \mathbf{n} &= 0 \qquad \text{on } [0,1], \\ \mathbf{n}' &= 0 \qquad \text{on } [0,1]. \end{aligned}$$

We assume there to be an energy functional W such that $\mathbf{n} = \partial W/\partial \mathbf{v}$ and $\mathbf{m} = \partial W/\partial \mathbf{u}$. Existence of solutions for this model has been shown in [12], but note that solutions may be nonunique.

We will couple the rod model to a linear elastic continuum. Let Ω be a domain in $\mathbb{R}^3$. Its boundary $\partial\Omega$ is supposed to be Lipschitz and to consist of disjoint parts

R. Bank et al. (eds.), *Domain Decomposition Methods in Science and Engineering XX*,
Lecture Notes in Computational Science and Engineering 91,
DOI 10.1007/978-3-642-35275-1_52, © Springer-Verlag Berlin Heidelberg 2013

Γ_N and Γ_D such that $\partial\Omega = \overline{\Gamma}_N \cup \overline{\Gamma}_D$ and Γ_D has positive two-dimensional measure. We use $\boldsymbol{\nu}_\Omega$ to denote the outward unit normal of Ω. For any displacement function $\mathbf{u} \in \mathbf{H}^1(\Omega) = (H^1(\Omega))^3$ we set $\boldsymbol{\varepsilon} = \frac{1}{2}(\nabla\mathbf{u} + \nabla\mathbf{u}^T)$ the linear strain tensor and the stress $\boldsymbol{\sigma} = \boldsymbol{\sigma}(\boldsymbol{\varepsilon})$, with a St. Venant–Kirchhoff-type material law

$$\boldsymbol{\sigma}(\boldsymbol{\varepsilon}) = \frac{E\nu}{(1+\nu)(1-2\nu)}(\operatorname{tr}\boldsymbol{\varepsilon})\mathrm{Id} + \frac{E}{1+\nu}\boldsymbol{\varepsilon}.$$

The parameters E and ν are the Young's modulus and Poisson ratio, respectively. The boundary value problem of elasticity is then

$$\begin{aligned} -\operatorname{div}\boldsymbol{\sigma}(\mathbf{u}) &= \mathbf{f} && \text{in } \Omega, \\ \mathbf{u} &= 0 && \text{on } \Gamma_D, \\ \boldsymbol{\sigma}(\mathbf{u})\boldsymbol{\nu}_\Omega &= \mathbf{t} && \text{on } \Gamma_N, \end{aligned}$$

with volume forces $\mathbf{f} : \Omega \to \mathbb{R}^3$ and surface force $\mathbf{t} : \Gamma_N \to \mathbb{R}^3$.

2 Coupling Conditions

We will now derive conditions for the coupling of a Cosserat rod and a linear elastic three-dimensional object. The two main difficulties are the difference in dimensions between the rod and the continuum, and the nonlinear nature of the rod configuration space.

Previous work has mainly focused on coupling linear models of different dimensions. Lagnese et al. [7] have studied the coupling of beams to plates extensively. Modeling of 3d–2d junctions between linear elastic objects using a method of asymptotic expansion has been carried out by Ciarlet et al. [4]. Monaghan et al. [8] describe a 3d–1d coupling between linear elastic elements in the discrete setting. A general framework which encompasses these cases is given in [3]. We are not aware of previous work on the coupling of Cosserat rods.

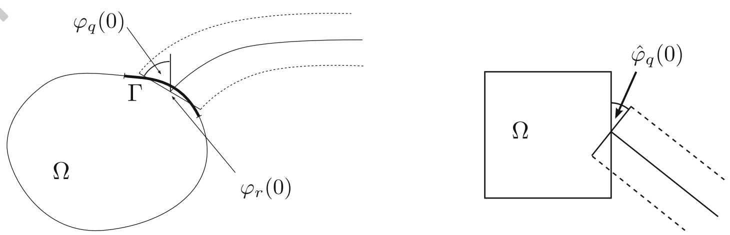

Fig. 1. *Left*: Coupling between a two-dimensional domain and a rod. *Right*: In the stress-free configuration the rod may meet the body at an arbitrary spatial angle $\hat{\varphi}_q(0)$

Consider again a linear elastic continuum defined on a reference configuration Ω. This time, the boundary $\partial\Omega$ is supposed to consist of three disjoint parts Γ_D, Γ_N,

UNCORRECTED PROOF

and Γ such that $\partial\Omega = \overline{\Gamma}_D \cup \overline{\Gamma}_N \cup \overline{\Gamma}$. We assume that Γ_D and Γ have positive two-dimensional measure. The three-dimensional object represented by Ω will couple with the rod across Γ, which we call the coupling boundary. The boundary of the parameter domain $[0,1]$ of a Cosserat rod consists only of the two points 0 and 1, and the respective domain normals are $\boldsymbol{\nu}_{r,0} = -1$ and $\boldsymbol{\nu}_{r,1} = 1$. To be specific, we pick 0 as the coupling boundary. We assume a stress-free rod configuration $\hat{\varphi} : [0,1] \to \mathrm{SE}(3)$ such that $\hat{\varphi}_r(0) = |\Gamma|^{-1} \int_\Gamma x\,ds$, i.e., the coupling interface of the rod in its stress-free state is placed at the center of gravity of the coupling interface of Ω. The orientation $\hat{\varphi}_q(0)$ of the stress-free state does not need to be in any relation with the shape of the coupling boundary Γ (Fig. 1).

We define our coupling using a set of conditions for the primal variables. These variables are the configuration φ of the rod and the displacement field $\mathbf{u}$ of the continuum. It is well known that when coupling two continuum models of the same type, the solution has to be continuous [9]. Since the position $\varphi_r(0) \in \mathbb{R}^3$ of the coupling cross-section can be seen as an averaged position it is natural to couple it to the averaged position of Γ

$$\varphi_r(0) \stackrel{!}{=} \frac{1}{|\Gamma|} \int_\Gamma (\mathbf{u}(x) + x)\,ds. \tag{1}$$

To obtain a complete set of primal conditions we also need to relate the orientations at the interface. This requires some technical preparations. Using the deformation gradient $F(\mathbf{u}) = \boldsymbol{\nabla}(\mathbf{u} + \mathrm{Id})$ we first define the average deformation of the interface boundary Γ as $\mathscr{F}(\mathbf{u}) = |\Gamma|^{-1} \int_\Gamma \boldsymbol{\nabla}(\mathbf{u}(x) + x)\,ds$. If $\mathbf{u}$ stays within the limits of linear elasticity the matrix $\mathscr{F}(\mathbf{u})$ has a positive determinant. Using the polar decomposition it can then be split into a rotation $\mathrm{polar}(\mathscr{F}(\mathbf{u}))$ and a stretching. We define the average orientation of Γ induced by a deformation $\mathbf{u}$ as the rotational part of $\mathscr{F}(\mathbf{u})$. This corresponds to the definition of the continuum rotation used in the theory of Cosserat continua. In particular, if $\mathbf{u} \equiv 0$ then $\mathrm{polar}(\mathscr{F}(\mathbf{u})) = \mathrm{Id}$.

The average orientation $\mathrm{polar}(\mathscr{F}(\mathbf{u}))$ can now be set in relation to $\varphi_q(0)$, the orientation of the rod cross-section at $s = 0$. We require the coupling condition to be fulfilled by the stress-free configuration $\mathbf{u} = 0$, $\varphi = \hat{\varphi}$. This leads to the condition

$$\varphi_q(0) \stackrel{!}{=} \mathrm{polar}(\mathscr{F}(\mathbf{u}))\hat{\varphi}_q(0), \tag{2}$$

which is an equation in the nonlinear three-dimensional space SO(3).

For ease of writing we will introduce the averaging operator $\mathrm{Av} : \mathbf{H}^1(\Omega) \to \mathrm{SE}(3)$ by setting

$$\mathrm{Av}(\mathbf{u}) = \Big(\frac{1}{|\Gamma|} \int_\Gamma (\mathbf{u}(x) + x)\,ds,\ \mathrm{polar}(\mathscr{F}(\mathbf{u}))\hat{\varphi}_q(0) \Big), \tag{3}$$

where we have used $(\cdot,\cdot)$ to denote elements of the product space $\mathrm{SE}(3) = \mathbb{R}^3 \rtimes \mathrm{SO}(3)$. It is a nonlinear generalization of the restriction operator used in [3]. Then (1) and (2) can be written concisely as

$$\varphi(0) \stackrel{!}{=} \mathrm{Av}(\mathbf{u}). \tag{4}$$

Note that we do not assume that Γ has the same shape or area as the rod cross-section at $s = 0$. Also, since the coupling conditions relate only finite-dimensional quantities

UNCORRECTED PROOF

they remain the same when the subdomain problems are replaced by finite element approximations.

The coupling problem is made complete by conditions for the dual variables. For the continuum these variables are the normal stresses at the boundary Γ. For the rod the dual variables are the total force $\mathbf{n}(0)\boldsymbol{\nu}_{r,0}$ and the total moment $\mathbf{m}(0)\boldsymbol{\nu}_{r,0}$ about $\varphi_r(0)$ transmitted in normal direction across the cross-section at $s=0$. We expect these to match the total force and torque exerted by the continuum across the coupling boundary Γ in the direction of $-\boldsymbol{\nu}_\Omega$

$$\int_\Gamma \boldsymbol{\sigma}(\mathbf{u})\boldsymbol{\nu}_\Omega\, ds = -\mathbf{n}(0)\boldsymbol{\nu}_{r,0} \tag{5}$$

$$\int_\Gamma (x-\varphi_r(0)) \times (\boldsymbol{\sigma}(\mathbf{u})\boldsymbol{\nu}_\Omega)\, ds = -\mathbf{m}(0)\boldsymbol{\nu}_{r,0}. \tag{6}$$

Together, these equations relate quantities in the six-dimensional space $T^*_{\varphi(0)}\mathrm{SE}(3)$.

Remark 1. A variational formulation suggests that (5) and (6) are not the dual conditions of (4) (cf. to [3] for the linear case). Together with (10), however, they are sufficient to construct a working solution algorithm.

3 A Dirichlet–Neumann Algorithm

In this section we present a Dirichlet–Neumann algorithm for the coupled problem. It can be interpreted as a fixed-point iteration for an equation on the trace space of the rod configuration space at $s=0$, i.e. on SE(3). Each iteration consists of three steps: a Dirichlet problem for the rod, a Neumann problem for the body, and a damped update along geodesics on SE(3). Let $\lambda^0 \in \mathrm{SE}(3)$ be the initial interface value and $k \geq 0$ the iteration number. In more detail, the steps are as follows.

1. *Dirichlet problem for the Cosserat rod*
   Let $\lambda^k, \varphi_D \in \mathrm{SE}(3)$ be the current interface value and a Dirichlet boundary value, respectively. Find a solution φ^{k+1} of the Dirichlet rod problem

$$\begin{aligned}
(\mathbf{m}^{k+1})' + (\varphi_r^{k+1})' \times \mathbf{n}^{k+1} &= 0 &\qquad &\text{on } [0,1]\\
(\mathbf{n}^{k+1})' &= 0 & &\text{on } [0,1]\\
\varphi^{k+1}(0) &= \lambda^k\\
\varphi^{k+1}(1) &= \varphi_D.
\end{aligned}$$

2. *Neumann problem for the continuum*
   The new rod iterate φ^{k+1} exerts a resultant force $\mathbf{n}^{k+1}(0)\boldsymbol{\nu}_{r,0}$ and moment $\mathbf{m}^{k+1}(0)\boldsymbol{\nu}_{r,0}$ across its cross-section at $s=0$. Construct a Neumann data field $\boldsymbol{\tau}^{k+1} : \Gamma \to \mathbb{R}^3$ such that

$$\int_\Gamma \boldsymbol{\tau}^{k+1}(x)\, ds = -\mathbf{n}^{k+1}(0)\boldsymbol{\nu}_{r,0} \tag{7}$$

UNCORRECTED PROOF

and

$$\int_{\Gamma}(x-\varphi_r^{k+1}(0))\times\boldsymbol{\tau}^{k+1}(x)\,ds=-\mathbf{m}^{k+1}(0)\boldsymbol{\nu}_{r,0}. \tag{8}$$

Then solve the three-dimensional linear elasticity problem with Neumann data $\boldsymbol{\tau}^{k+1}$ on Γ

$$\begin{aligned} -\operatorname{div}\boldsymbol{\sigma}(\mathbf{u}^{k+1}) &= \mathbf{f} && \text{in } \Omega \\ \boldsymbol{\sigma}(\mathbf{u}^{k+1})\boldsymbol{\nu}_{\Omega} &= \boldsymbol{\tau}^{k+1} && \text{on } \Gamma \\ \mathbf{u}^{k+1} &= 0 && \text{on } \Gamma_D \\ \boldsymbol{\sigma}(\mathbf{u}^{k+1})\boldsymbol{\nu}_{\Omega} &= \mathbf{t} && \text{on } \Gamma_N. \end{aligned} \tag{9}$$

3. *Damped geodesic update*
From the solution $\mathbf{u}^{k+1}$ compute the average interface displacement and orientation $\mathrm{Av}(\mathbf{u}^{k+1})$ as defined in (3). With a damping parameter $\theta > 0$, the new interface value λ^{k+1} is then computed as a geodesic combination in SE(3) of the old value λ^k and $\mathrm{Av}(\mathbf{u}^{k+1})$,

$$\lambda^{k+1}=\exp_{\lambda^k}\theta\left[\exp_{\lambda^k}^{-1}\mathrm{Av}(\mathbf{u}^{k+1})\right].$$

It remains to say how to construct suitable fields of Neumann data $\boldsymbol{\tau}^{k+1}$ that satisfy the conditions (7) and (8). Let us drop the index k for simplicity. In principle, any function $\boldsymbol{\tau}:\Gamma\to\mathbb{R}^3$ of sufficient regularity fulfilling (7) and (8) can be used as Neumann data in (9). It has been shown in [10] that such functions exist.

The theory of Cosserat rods assumes that forces and moments are transmitted evenly across cross-sections. We therefore construct $\boldsymbol{\tau}$ to be 'as constant as possible'. More formally, we introduce the functional

$$T:\mathbf{L}^2(\Gamma)\times\mathbb{R}^3\to\mathbb{R}, \qquad T(\mathbf{h},\mathbf{c})=\int_{\Gamma}\|\mathbf{h}(x)-\mathbf{c}\|^2\,ds,$$

and construct $\boldsymbol{\tau}$ as the solution of the minimization problem

$$(\boldsymbol{\tau},\mathbf{c}_{\boldsymbol{\tau}})=\operatorname*{arg\,min}_{\mathbf{h}\in\mathbf{L}^2(\Gamma),\,\mathbf{c}\in\mathbb{R}^3} T(\mathbf{h},\mathbf{c}) \tag{10}$$

under the constraints that

$$\int_{\Gamma}\boldsymbol{\tau}\,ds=-\mathbf{n}(0)\boldsymbol{\nu}_{r,0} \qquad \text{and} \qquad \int_{\Gamma}(x-\varphi_r(0))\times\boldsymbol{\tau}\,ds=-\mathbf{m}(0)\boldsymbol{\nu}_{r,0}. \tag{11}$$

Problem (10) and (11) is a convex minimization problem with linear equality constraints. In [10, Lemma 5.3.4] it was shown that there exists a unique solution. In a finite element setting the problem size is given by the number of grid vertices on Γ times 3. A minimization problem of this type can be solved, e.g., with an interior-point method.

UNCORRECTED PROOF

this figure will be printed in b/w

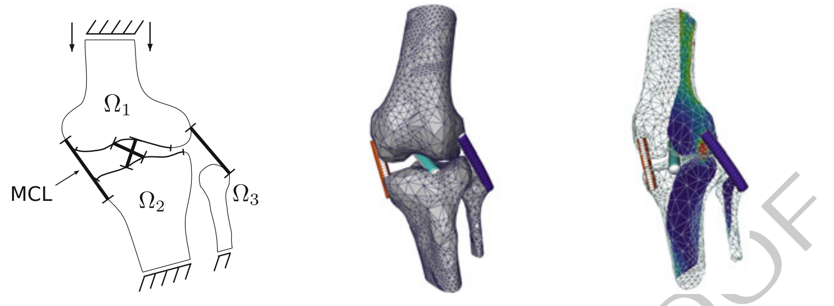

Fig. 2. *Left*: Problem setting. Tibia and fibula are rotated 15° in valgus direction to put additional stress on the MCL. *Center*: Deformed grids after two adaptive refinement steps. *Right*: Two sagittal cuts through the von Mises stress field

4 Numerical Results

We close with a simulation result for a knee model which combines femur, tibia, and fibula bones modeled as three-dimensional linear elastic objects, and the cruciate and collateral ligaments, modeled as Cosserat rods. The model additionally includes the contact between femur and tibia. To obtain a test case where the contact stresses do not entirely predominate the stresses created in the bone by pulling ligaments, we applied a valgus rotation of 15° to tibia and fibula. This leads to a high strain in the medial collateral ligament (MCL) and can be interpreted as an imminent MCL rupture (Fig. 2).

The geometry was obtained from the Visible Human data set. We modeled bone with an isotropic, homogeneous, linear elastic material with $E = 17\,\text{GPa}$ and $\nu = 0.3$. The distal horizontal sections of tibia and fibula were clamped, and a prescribed downward displacement of 2 mm was applied to the upper section of the femur. We used first-order finite elements for the discretization of the linear elasticity problem. DUNE [2] was used for the implementation.

The four ligaments were each modeled by a single Cosserat rod with a circular cross-section of radius 5 mm. The rod equations were discretized using geodesic finite elements [11]. We chose a linear material law (see, e.g., [6]) with parameters $E = 330\,\text{MPa}$ and $\nu = 0.3$. On the bones, the coupling boundaries Γ for the different ligaments were marked by hand using a graphical editor. We modeled all ligaments to be straight in their stress-free configurations and to have 8 % in situ strain.

We solved the combined problem using the Dirichlet–Neumann algorithm described in Sect. 3. At each iteration, a pure Dirichlet problem had to be solved for each of the rods and a contact problem with mixed Dirichlet–Neumann boundary conditions had to be solved for the bones. The contact problem was solved using the Truncated Nonsmooth Newton Multigrid (TNNMG) algorithm [5]. The TNNMG method solves linear contact problems with the efficiency of linear multigrid. For the ligaments we used a Riemannian trust-region solver [1, 11], and we used IPOpt [13] to solve the minimization problems (10) and (11). Figure 2 shows the deformed con-

UNCORRECTED PROOF

this figure will be printed in b/w

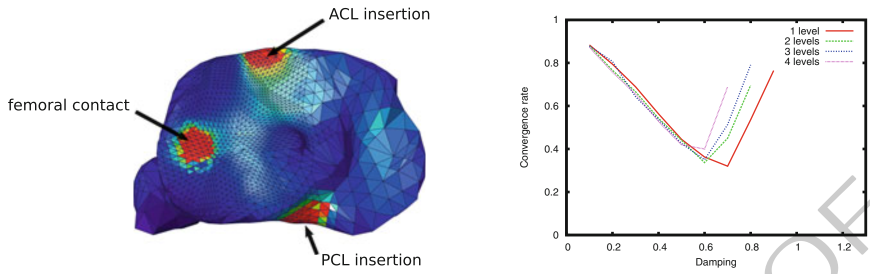

Fig. 3. *Left*: Stress plot on the tibial plateau. *Right*: Convergence rates of the Dirichlet–Neumann method as a function of the damping parameter for up to four grid levels

figuration on a grid obtained by two steps of adaptive refinement and cuts through the von Mises stress field. In Fig. 3, left, a caudal view onto the tibial plateau can be seen, which is colored according to the von Mises stress. The peaks due to contact and the pull of the cruciate ligaments can be clearly observed.

We measured the Dirichlet–Neumann convergence rates with bone grids obtained by up to three steps of adaptive refinement using the hierarchical error estimator presented in [10]. Rod grids in turn were refined uniformly. On each new set of grids we started the computation from the reference configuration. That way identical initial iterates for all grid refinement levels were obtained. Details on the measuring setup can be found in [10]. Figure 3, right, shows the Dirichlet–Neumann convergence rates plotted as a function of the damping parameter θ for up to four levels of refinement. For each further level of refinement, the optimal convergence rate is slightly worse than for the previous, and obtained for a slightly lower damping parameter. This behavior seems typical for Dirichlet–Neumann methods. Nevertheless the optimal convergence rates stay around 0.4. This makes the algorithm well usable in practice.

Bibliography

[1] P.-A. Absil, C. G. Baker, and K. A. Gallivan. Trust-region methods on Riemannian manifolds. *Found. Comput. Math.*, 7(3):303–330, 2007.

[2] P. Bastian, M. Blatt, A. Dedner, C. Engwer, R. Klöfkorn, R. Kornhuber, M. Ohlberger, and O. Sander. A generic interface for parallel and adaptive scientific computing. Part II: Implementation and tests in DUNE. *Computing*, 82(2–3):121–138, 2008.

[3] P. J. Blanco, M. Discacciati, and A. Quarteroni. Modeling dimensionally-heterogenenous problems: analysis, approximation and applications. Technical Report 14, MATHICSE, 2010.

[4] P. G. Ciarlet, H. LeDret, and R. Nzengwa. Junctions between three-dimensional and two-dimensional linearly elastic structures. *J. Math. Pures Appl.*, 68:261–295, 1989.

UNCORRECTED PROOF

[5] C. Gräser, U. Sack, and O. Sander. Truncated nonsmooth Newton multigrid methods for convex minimization problems. In *Proc. of DD18*, LNCSE, pages 129–136. Springer, 2009.

[6] S. Kehrbaum. *Hamiltonian Formulations of the Equilibrium Conditions Governing Elastic Rods: Qualitative Analysis and Effective Properties*. PhD thesis, University of Maryland, 1997.

[7] J. Lagnese, G. Leugering, and E. Schmidt. *Modeling, Analysis and Control of Dynamic Elastic Multi-Link Structures*. Birkhäuser, 1994.

[8] D. J. Monaghan, I. W. Doherty, D. M. Court, and C. G. Armstrong. Coupling 1D beams to 3D bodies. In *Proc. 7th Int. Meshing Roundtable*. Sandia National Laboratories, 1998.

[9] A. Quarteroni and A. Valli. *Domain Decomposition Methods for Partial Differential Equations*. Oxford Science Publications, 1999.

[10] O. Sander. *Multidimensional Coupling in a Human Knee Model*. PhD thesis, Freie Universität Berlin, 2008.

[11] O. Sander. Geodesic finite elements for Cosserat rods. *Int. J. Num. Meth. Eng.*, 82(13):1645–1670, 2010.

[12] T. I. Seidman and P. Wolfe. Equilibrium states of an elastic conducting rod in a magnetic field. *Arch. Rational Mech. Anal.*, 102:307–329, 1988.

[13] A. Wächter and L. T. Biegler. On the implementation of a primal–dual interior point filter line search algorithm for large-scale nonlinear programming. *Math. Progr.*, 106(1):25–57, 2006.

UNCORRECTED PROOF